Compression System

Data Compression State of the Art and Compression Experiments

March 2021

Miguel Hernández-Cabronero

Ashwin Kumar

Joan Serra-Sagristà

Universitat Autònoma de Barcelona

TABLE OF CONTENTS

Table of Contents

ABSTRACT

This document describes the different activities conducted by the Universitat Autònoma de Barcelona on the the Retos Colaboración RTC2019-007434-7 project. These are for the most part related to work package 1 “Definition and scope”, and 3 “Compression system”.

An introduction to satellite constellations from the general perspective of the project is provided first. The reader will find general contextual information, useful to understand the remaining sections.

A review of the state of the art on satellite constellation data compression is provided next. Several well-defined, peer-reviewed approaches are described here, which will be considered in later stages of the compression system development.

Results for a set of exploratory experiments are presented afterwards. A study run of the test data suggest that compressing each horizontal region separately may produce improved compression results. Several low-complexity compression algorithms are analyzed, jointly in terms of the compression efficiency and time complexity results.

In light of the obtained results, the recommended path of action for this project’s compression system is to employ custom V2F codes to leverage their exceptional time performance, with expected improvements upon the Marlin V2F compressor.

INTRODUCTION

A single satellite in a GEO (geosynchronous orbit) above the equator cannot see more than 30% of the Earth's surface [1]. For global or near-global coverage, you need several satellites – a satellite constellation.

The primary advantage that a LEO (low earth orbiting) satellite constellation has over less complex but much bigger and expensive higher-altitude systems (geostationary) with fewer operational satellites is the ability to reuse the available communication frequencies in an increased number of separated areas across the earth’s surface. This reuse of available spectrum allocation leads to a far higher simultaneous transmission abilities and thus much higher system capacities. This increased system capacity is very important from a commercial standpoint as it helps maximise revenue in an industry which has steep capital expenditure and a high failure rate. The movement of LEO and MEO (medium earth orbiting) satellites relative to the Earth's surface means that a number of satellites have to be launched and made operational before continuous coverage of, and commercial service to, an area become possible [2]

Along with providing near global-coverage LEO and MEO satellite constellations can have significantly lower communication latency compared to geostationary satellites [3]. The LEO satellite constellations can also provide significantly better spatial and temporal resolution of the target, along with huge cost savings across the board.

SATELLITE CONSTELLATIONS

Simply stated a satellite constellation is a group of satellites working together to achieve a single purpose. This network of small satellites should be able to operate symbiotically.

Small satellites, deployed as a sensor network in space, have an advantage over conventional satellites in space exploration because of their low-cost access to space. They significantly reduce the cost barrier of entry and have certain technical advantages over the bigger geostationary satellites, such as lower revisit times, higher coverage with the help of multiple satellites, lower latency due to proximity to the earth, lower cost of development due to the ability to use commercial off-the-shelf components (COTS), ability to mass-produce and shorter lead times.

Type of satellite	**Mass**
Minisatellite	500-100kg
Microsatellite	100-10kg
Nanosatellite (CubeSats)	10-1kg
Femto and Pico-satellite	<1kg

Table 1 Small spacecraft classification

Another important reason for the shift from expensive GEO satellites to low-cost LEO satellites is the inherent capability of distributed multi-satellite nodes, which has potential for autonomous operations, distributed processing and proximity operations. Several small satellites flying in a formation would collaboratively achieve the mission aim at lower cost and with enhanced reliability and efficiency compared to larger single platform mission. To enable cooperation among these distributed multi-satellite nodes requires a need for inter-satellite communication (ISC) [4].

This chapter aims at studying the various areas of research focused on LEO satellite constellations. The primary research area in the early 2000s regarding satellite constellations was on the orbits and on how to arrange these constellations to put available resources into best use. Then papers on collision avoidance and collision mapping and visualisation of the constellations started appearing. These dealt with not only on how to structure the constellation but also on how different constellations might affect one another and on how to deal with these issues. And at present, the main area of research focus is on how to enable seamless communication (between these satellites in a constellation), which we´ll take a deeper look in the next chapter. Let us look at each of these research areas in brief:

Orbits and formations:

The design of satellite constellations highly depends on orbital mechanics and resulting satellite geometry. This geometry affects a lot of factors such as coverage area, visibility of satellites to the ground terminals and the most important: the ever-changing network topology.

When satellites fly in formations, they need to maintain a set distance and orientation relative to one another to avoid collision and to accomplish mission objectives. There can be two primary approaches to maintain these formations: Ground-based control and autonomous control. In ground-based control the satellites relay information back to the ground station where the necessary calculations are made to manoeuvre the satellite into proper formation. While in autonomous control the satellites are in contact with one another and make the necessary calculations to stay in formation and proceed to carry out those manoeuvres with the help of altitude and orbit control systems onboard.

There are various types of formations the satellites can be in, which highly depends on mission requirements. The most common ones being:

a. Trailing: In this formation multiple satellites share a single orbit and follow each other at a specified time period to view a target at different time periods or to obtain varied viewing angles. It is also known as a string of pearls configuration.

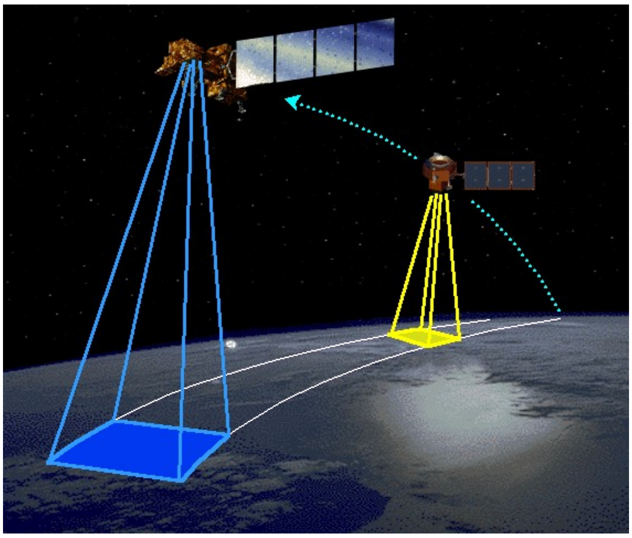

Figure 1: Landsat7 and EO-1 trailing

b. Cluster: In this formation a group of satellites will be deployed in their respective orbits and will stay in a dense arrangement. Often used when high resolution mapping is required.

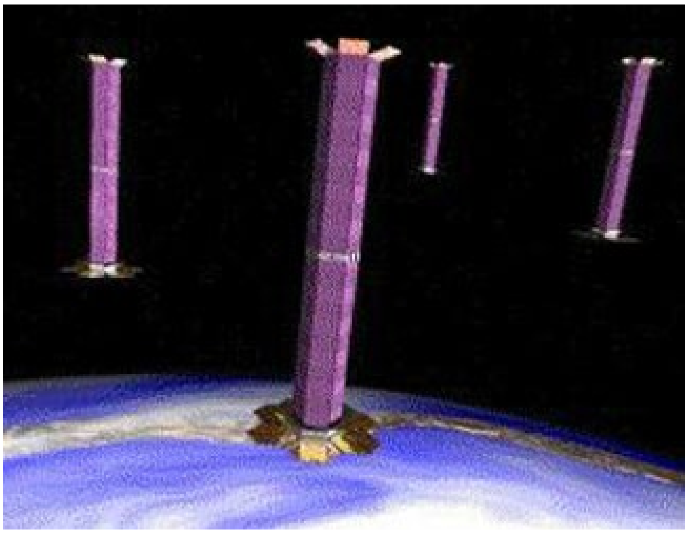

Figure 2 Cluster formation for the proposed TechSat-21 mission

c. Constellation: This formation consists of satellites in different orbital planes providing a very large area of coverage. They are coordinated and orchestrated such that the satellites in the system complement rather that interfere with one another.

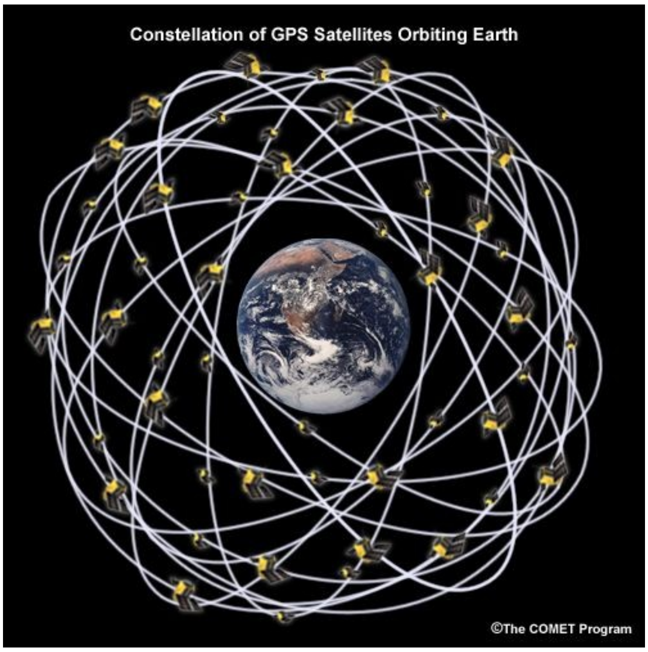

Figure 3 GPS Constellation

The constellation formation can be further classified based on the orbital planes, satellite spacing, inclination, eccentricity and a few other factors. Let's take a brief look at the most common designs of LEO satellite constellation:

I. Walker constellation:

A class of circular orbit geometries that has become popular is the Walker Delta constellation. This has an associated notion: i: t/p/f

Where 'i' is the inclination; 't' is total number of satellites; 'p' is number of equally spaced planes; and 'f' is relative spacing between satellites in adjacent planes. E.g.: The Galileo Navigation System is a Walker Delta 56°:24/3/1 constellation [5].

There is another set of Walker constellation called the Walker Star. Where the satellites are in a near polar orbit. E.g.: The Iridium constellation form a Walker Star of 86.4°:66/6/2 [6]

II. Rosette:

Provides the best coverage at mid-latitudes where there is a significant chunk of the human population but provides poor coverage near the poles.

III. Polar

These are based on the view of their orbits from a pole. With inter-satellite links these form variants of toroidal networks. New formations are being researched where each proposal has its strength and weakness. Varying the factors such as revisit times, area of coverage, no. of satellites required, obtainable data from the satellites, upload windows, hand over at the seam, no. of ground terminals with varying results.

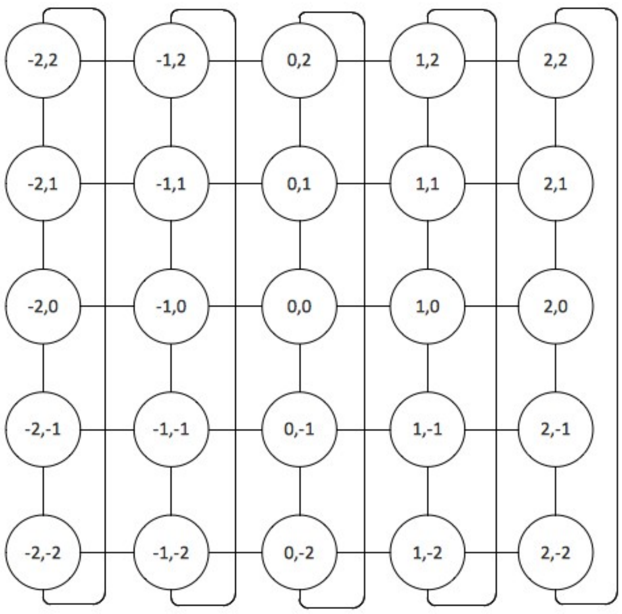

Figure 4 Toroidal Network Topology

Few papers discuss the reconfiguration of satellite constellation based on their purpose (EO or disaster response) [7].

Collision avoidance, collision mapping and visualization of the constellations

Collision avoidance is a topic with increasing importance in the aerospace community since the collision of the Cosmos 2251 and Iridium 33 satellite and mathematic models for debris assessment and risk mitigation are refined [8]. Subsequently, appropriate methods have been researched to potentially mitigate these incidents with light and inexpensive onboard equipment.

Satellite constellations are subjected to a myriad of changing space conditions (such as radiation, solar flux, change in the orbit due to the gravity, etc) and various avoidance and orbit maintenance manoeuvres can be performed to overcome these difficulties [9].

INTER SATELLITE COMMUNICATION

The overall architecture for Inter Satellite Communication (ISC) can be described using the OSI (Open System Interconnection) or its derivatives as presented in [4],[10][11], [12]. For small satellite systems the upper few layers can be merged as shown in the following figure which can then be controlled by software.

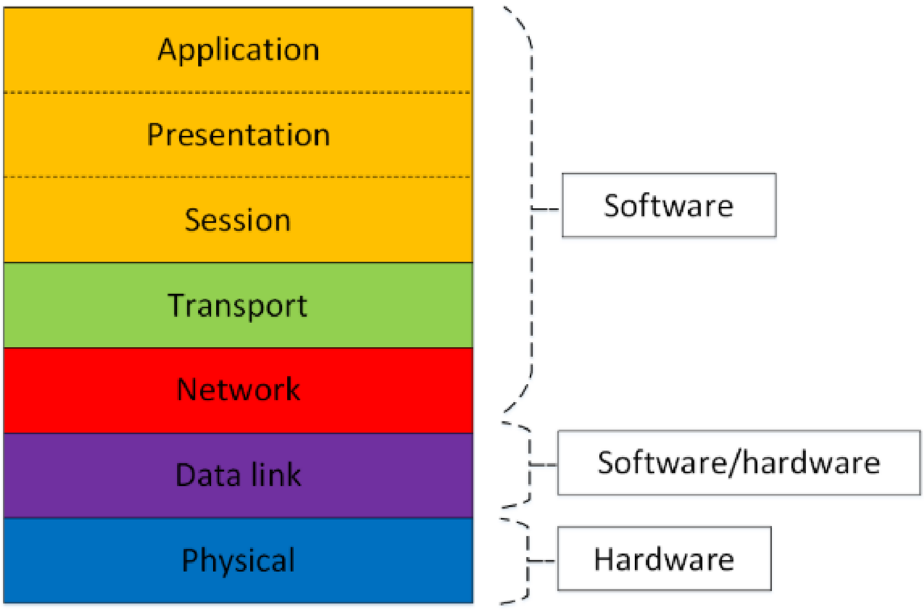

Techniques used for implementing inter-satellite communication links (ISLs) consist of using either radiofrequency (RF) or various methods of optical communication (Lasers, Visible light). This area is not further discussed in this report, as it is not as directly related to the tasks at hand.

STATE OF THE ART ON SATELLITE DATA COMPRESSION

As of now, there seems to be not much research publicly available on satellite constellation data compression. There is heavy research in the field of satellite data compression wherein, data is compressed onboard the satellite and then sent to the ground station for processing, and various compression standards and schemas focusing on this area while research on satellite constellation systems where we could further exploit the properties of multiple close satellites to achieve higher compression with the help of inter-satellite links is just beginning. We present a brief review on the current literature available related to satellite constellation data compression in this chapter.

Aulí-Llinàs et al. [13] proposed a coding scheme for EO in which they suggest uploading a quantized reference image generated using historical images using the uplink bandwidth (making the best use of the full duplex capacity of the communication channel) and exploiting this temporal redundancy to achieve higher compression. They suggest making use of the redundancy in the repeat cycle (when the satellite comes back to its starting point and scan areas that were already captured in the previous cycle) and the heavy processing and storage capabilities of the ground station to coregister the images with variations in the satellites position and direction. The novel idea they proposed was to use the historical images already captured to generate a reference image which will then be coded and transmitted to the satellite with the uplink bandwidth which is then decoded by the satellite and used to compress the image it captures which would be sent via the downlink channel. They were able to get gains of up to 0.5 bps (bits per sample) for lossless compression and significant image quality gains of up to 10 dB for lossy compression.

They further expand this work in [14] by taking into consideration the practical and synchronization aspects of the proposed dual link image coding (DLIC) technique. Their proposed implementation model is as follows: Take the reference image (Y) and wavelet transform this image as higher efficiency of entropy-based techniques are achieved in the wavelet domain instead of the image domain. Then they use a JPEG2000 encoder to encode this image ($\hat{Y}$) and this code stream is sent to the satellite via the uplink channel. The satellite wavelet transforms the captured image (X), and after partially decoding the code stream $\hat{Y}$ starts computing the residual image (R) using the wavelet transformed captured image (X) and $\hat{Y}$. This residual image is then encoded ($\hat{R}$) and sent to the ground station via the downlink channel which is then decoded in the ground station and the recovered image ($\hat{X}$) is obtained after performing a inverse wavelet transform.

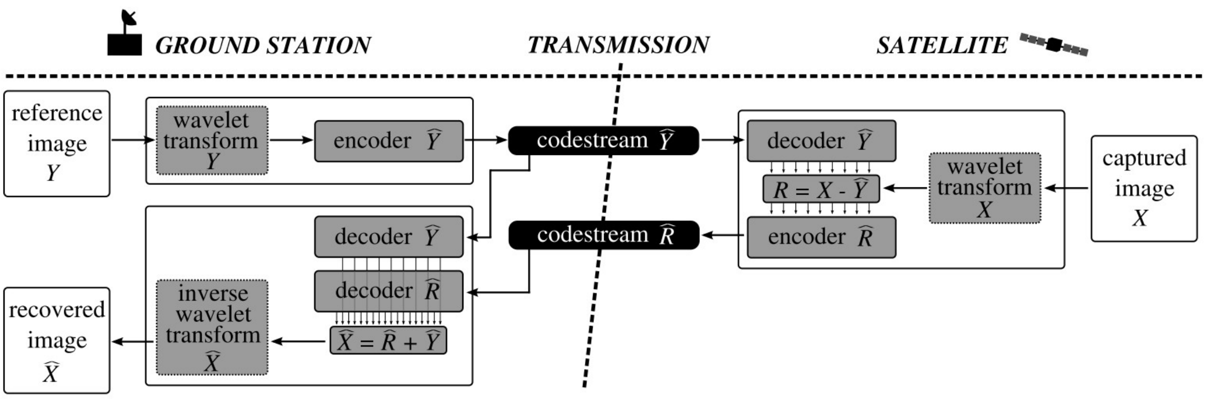

Figure 12 Practical Model to implement DLIC scheme

They propose 3 techniques to generate this reference image. The first of which being using the most recent captured image of that area, even though this sounds like a very simple method it is very effective because it captures the latest changes in that area and often the satellites revisit the area around the same time allowing for images with same illumination and other such properties which allows for higher compression. In the second method they propose an image averaging technique with a dataset of images up to 1 year in prior to this day or more. Handling meteorological events such as cloud becomes a difficult task because of their inherent randomness in such cases. The third technique they propose is to use the correlation between the images, although this is not practical as it can be performed only after capturing the said image it does provide a good metric from a theoretical perspective. They were able to obtain a coding gains of up to 0.8bps for lossless compression and up to 8dB for lossy compression on images which weren't affected due to meteorological events such as clouds, rain, snow, etc.

This approach could be further explored in terms of satellite constellation data compression wherein the entire satellite train in a particular orbit can benefit from the same reference image and achieve higher compression, or we could use multiple reference images based on the time of the day and weather conditions to achieve better similarity in illumination properties and meteorological information. The ability to share information between satellites using satellite links and the ability to upload data to any satellite, again using a ground-satellite link and then ISL can also be exploited for achieving higher compression. The trade-off between power and compression ratios using such a schema along with the communication and routing protocols could be studied further to analyse if an investment into ISL for the entire constellation would payoff in the long run.

Zhou et al. [15] proposed one such data scheduling scheme for small satellite networks (SSN). They propose a finite-embedded-infinite two-level dynamic programming framework with considerations of the practical issues of stochastic data arrival and time-varying IS contacts specifically in SSN environment. They propose two JFBI (Joint forwards and backward induction) algorithms, i.e., VB-JFBI (value based) and PB-JFBI (policy based) algorithms, to efficiently solve stochastic data scheduling optimization problem and further formulate this scheduling optimization problem as an MDP (Markov decision process) problem.

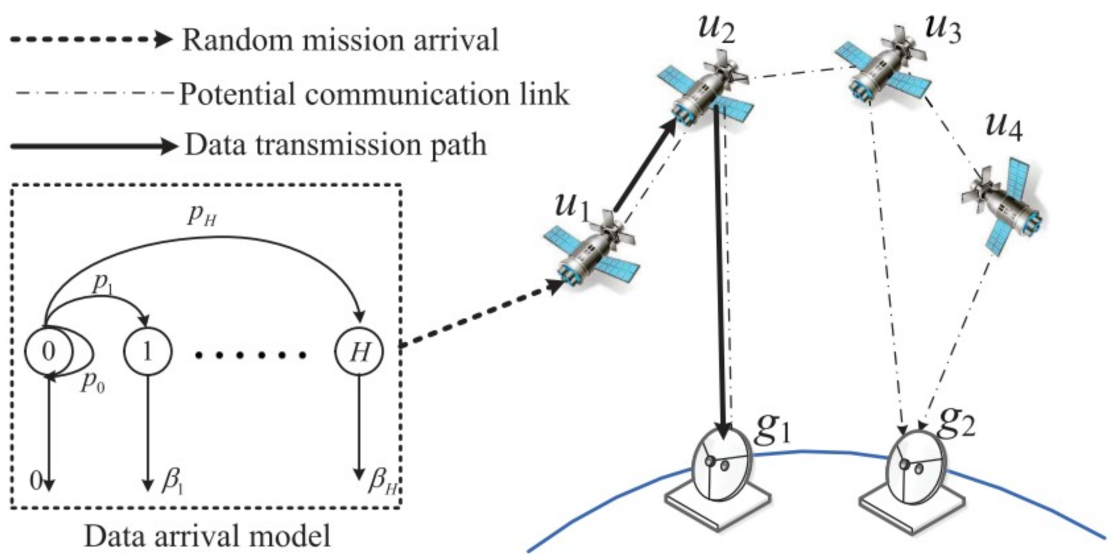

Figure 13 SSN model and data arrival model

Their proposed JFBI algorithms can generate the optimal contact selection policy in accordance with inter satellite channel condition, battery condition, and storage condition for any initial resource status.

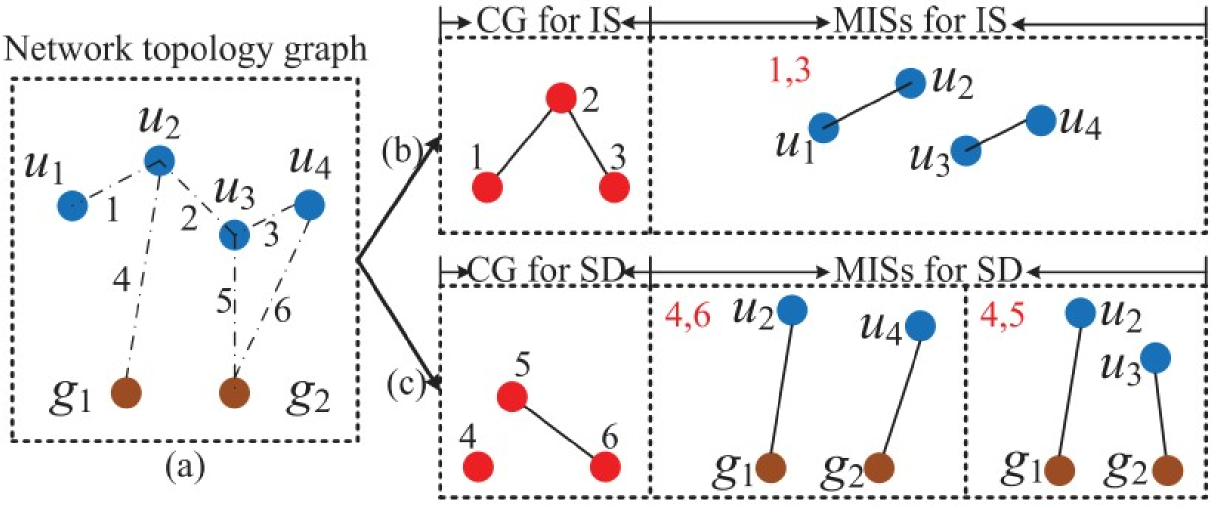

Figure 14 Maximum feasible inter satellite and satellite downlink contacts selection schematic

They provide insightful analysis on the impact of each associated factor such as storage capacity, battery, etc for different discounting factors.

Another interesting approach was the creative use of deep learning methods for image compression. Specifically, generative adversarial networks (GAN) and the variational auto encoder (VAE). GANs are an architectural model proposed by Ian et al. [16] where two networks the generator and discriminator compete against each other, thus adversarial. The role of the generator network is to take as input random variables of uniform probability distribution and use it to synthesize a random vector in the N dimensional vector space that follows a particular probability distribution (i.e. new data instances) which fool the discriminator, i.e. maximise the final classification error while on the other hand the discriminator network must predict if the generated vector (data instance) is real (from the actual domain) or fake (generated), i.e. minimise the classification error [17]. Both the networks try to beat other and inherently become better at their tasks.

GAN has been seeing a lot of research interest recently due to its multi-domain benefits and the ability to use it for image related applications where the result can be properly visualised. GANs can be used to generate extremely photorealistic images and are being used for image-to-image translation tasks.

The following figure illustrates such a model in action and how the data distribution is used to train the model further.

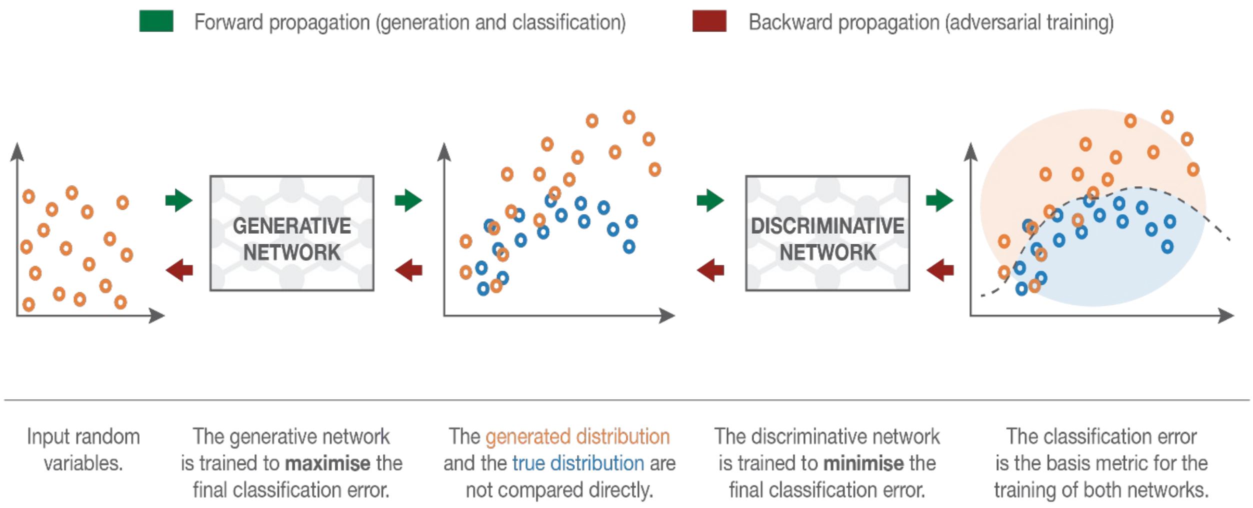

Figure 15 Generative Adversarial Network

VAEs are another interesting generative model. Autoencoders encode input data into a vector which compresses the original data and creates a new representation, often reducing the number of dimensions (features that describe data) which is later decoded by a decoder network the result of which is compared to the original data and the error is backpropagated to update network accordingly. This dimensionality reduction can be accomplished with feature selection (only important existing features are conserved) or by feature extraction wherein a lower number of new features are created based on the old features. Important trade-offs to be considered while generating such a network is the lack of regularity in the encoded vector space (latent space) along with a need to keep the major structural part of the data intact in the reduced representation.

Once the network is trained, we could use the decoder to generate new data by taking a point randomly from the latent space as its input. But this is not an easy task as despite the low dimensionality of the latent space there will often be severe overfitting thus some points of the latent space will give meaningless content once decoded.

Figure 16 Difference between a "regular" and an "irregular" latent space.

This issue can be overcome with the use of VAEs. In VAEs the latent space is normalized during the training to ensure that overfitting of data is avoided, and the latent space has some good properties/features which allows us to generate meaningful new data.

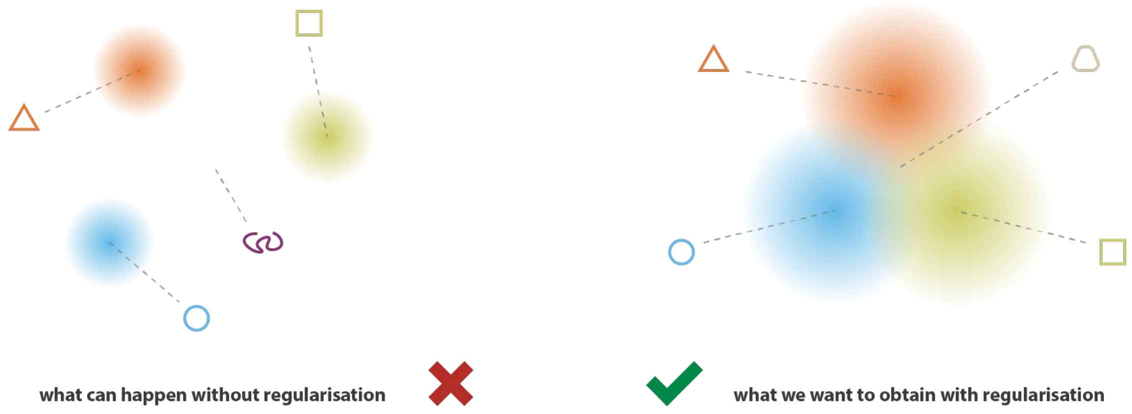

Figure 17 Normalized distribution in a VAE

Even though VAE and GAN seem to do the exact same task, data generated from GANs often tend be with more granular details while VAEs tend to generate more blurred output. This is not always the case and is highly dependent on the model, with recent research on VAE [18] indicating it could deliver similar results compared to state-of-the-art GAN models. On of the most popular applications for conditional GANs models are image-to-image translation tasks. Both GAN and VAE models have a one-to-one mapping and fail to output a diverse range of output images, which is needed for multi-modal image-to-image translation tasks. Gonzalez-Garcia et al. [19] proposes the concept of cross-domain disentanglement and a hybrid model that combines both GAN and cross-domain auto encoders to solve this issue.

Their model disentangles domain specific information from other features that are shared across different domains. Disentangling image specific features, such as difference in illumination, reflectance, shadows, viewpoint, tilt and object orientation from the intrinsic scene properties allows their model to be aware of isolated factors variation while preserving the underlying structural data. Therefore, models can marginalize information along a particular factor of variation, should it be not relevant for the task at hand. Moreover, disentangled representations grant a more precise control for those tasks that perform actions based on the representation. To do so they propose to split the information into two parts one shared representation containing features from both the domains and two exclusive representations that have features unique to each domain. They use a novel network component called a cross-domain autoencoder to achieve consistency across domains and to make sue the generated images correspond to the input. Their models are able to outperform state of the art models in multi-modal image translation and cross-domain image retrieval tasks.

Sanchez et al. [20] proposes a disentangled representation specifically for a satellite image time series. They were one of the first to apply such a deep learning model particularly for satellite images. They propose to disentangle the image data into two parts, one is a shared representation that captures common properties between the images and another an exclusive representation that contains specific information regarding each image in the time series. The shared representation aims to capture the underlying structure of the images. A combination of both would produce the original image back. Their cross-domain autoencoder model integrates VAE and GAN. This method performs well for various tasks such as image-to-image translation, multimodal generation, image classification, image retrieval, image segmentation and change detection. However, it often generates structural artefacts, which makes it difficult to apply it directly for generating reference images.

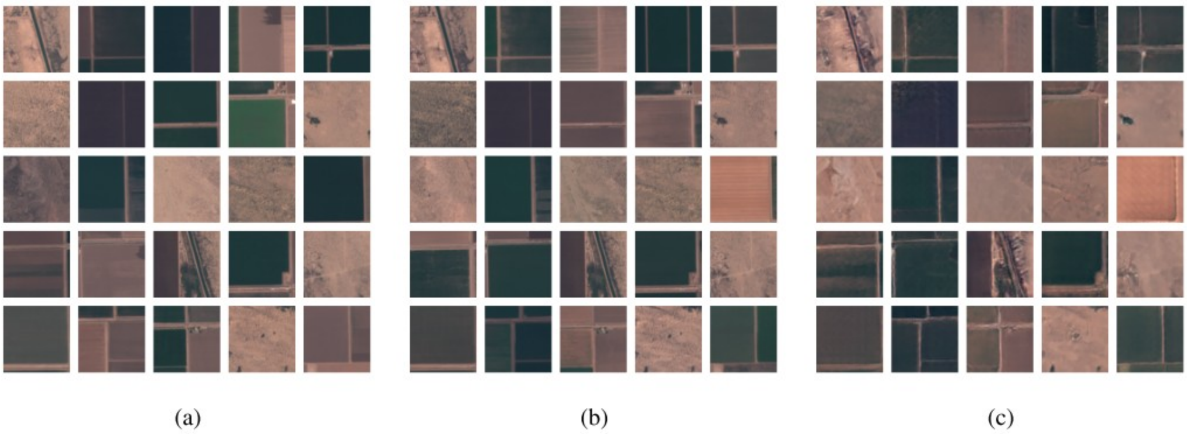

Figure 18 . Image translation performed on images of Brawley, California. (a) Images used to extract the shared features; (b) Images used to extract the exclusive features; (c) Generated images from the shared representation of (a) and the exclusive representation

Lirong et al. [21] proposes a GAN based compression schema which exploits several properties discussed above. GAN and VAE based models can, not only perform excellently for image-to-image translation and multi modal image generation tasks but can also deliver excellent results in image compression tasks which combined with their ability for multi-modal image generation opens several possibilities. Their proposed GAN based tunable compression model is able to compress images to any specific bits per pixel (bpp) based on the requirement without having to retrain the model for each case. They are able to outperform state-of-the-art models when bpp is very low by reconstructing non-important regions to compensate for the severe distortion that usually occurs at such levels due to insufficient allocation of bits in those regions. Their model outperforms the current state-of-the-art models when bpp is lower than 0.2.

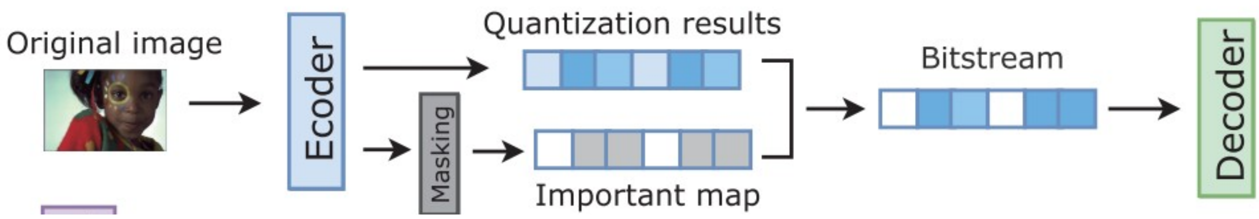

Figure 19 Proposed GAN based tunable compression model

Ze Cui et al. [22] proposes a G-VAE (Gained Variational Autoencoder) framework for a continuously variable rate image compression. Their model is not specifically tuned for satellite images but does emphasize the capabilities of VAE and GAN based compression models by outperforming all published results on Kodak datasets in both PSNR (Peak signal-to-noise-ratio) and MS-SSIM (Muti scale structural similarity) metrics and better compression than classical image codecs such as BPH which is a intra-frame encoding of the high efficiency video codec (HEVC)

GAN and other deep learning-based image compression schemes excel at their tasks but previously haven't been extensively used for onboard satellite data compression because they are computationally intensive tasks to be performed. Recent advances in this field such as the architecture proposed by Muyang et al. [23] allows for compressed Conditional GAN based systems to be deployed on edge devices. Their model is able to compress state-of-the-art conditional GAN based systems by up to 9-21x and reduce the model size by 5-33x without having any significant performance implications and also consistently improve performance in certain model sizes.

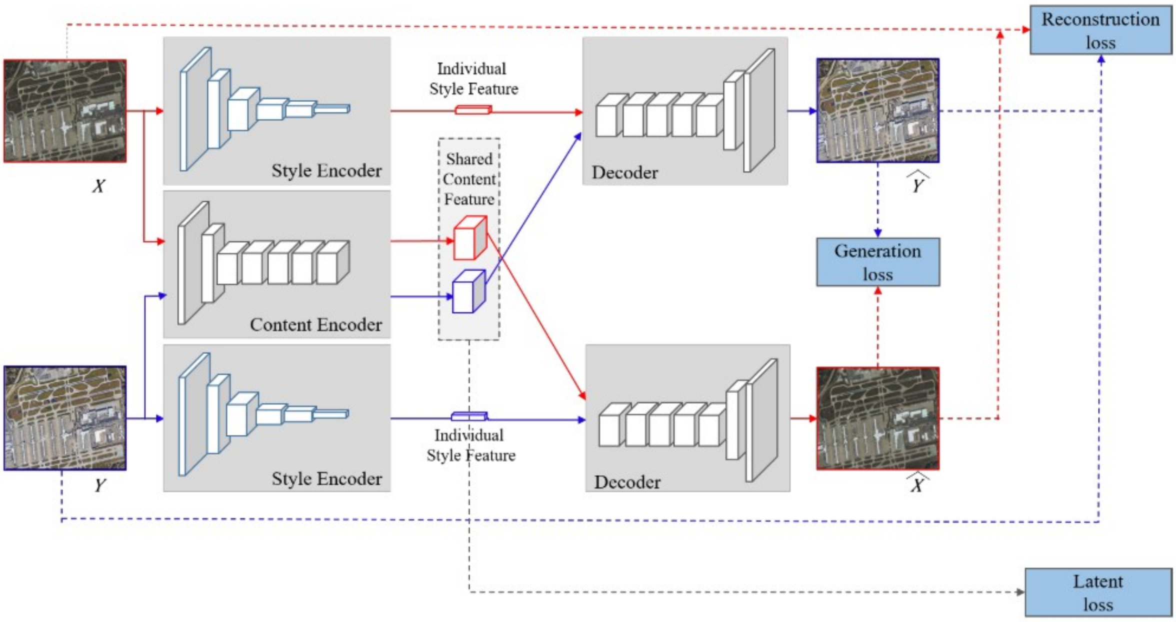

Liao et al. [24] offers a representation learning-based method for video satellite remote sensing. This network aims to model the evolution of the underlying landscape under different conditions by making use of historical image series. They propose an unsupervised disentangled representation learning network of the satellite image series where the description of the landscape is divided into two parts the content feature and the style feature. The content feature is shared between the images in a series (an image series is the collection of historical images of a particular location) and the style feature differentiates one image from the other in the series. The content feature contains the underlying structure of the image i.e. the consistent landscape of the image while the style feature contains info on the slight variations that would be present in images taken at different time slots i.e. the various environmental parameters. Unlike traditional approaches where only one image is used to represent the historical image data they utilize a series of historical images and image translation techniques to improve the quality of the image series. These synthetic reference frames can highly boost the compression efficiency by changing the original intra-frame prediction to inter-frame prediction for the intra-coded picture.

A video clip contains the intra-coded picture (I frame), predicted picture (P frame),and bidirectional predicted picture (B frame). Typically, the I frame is compressed by intra-frame coding, which costs a higher bitrate than inter-frame coding. The other two types of frame are usually compressed by inter-frame coding. Particularly for the satellite video, the spatial correlation is weak, while the long-term temporal correlation is strong due to the slowly moving background. Generally, the bitrate cost of the I frame is about 2–10 times over that of the P frame. Therefore, using the generated background reference as the reference frame to remove the LBR of I frames can significantly improve compression. When these frames are integrated into the proposed video compression scheme, they show significant bitrate savings of up to 44.22% on average over the main profile of HEVC.

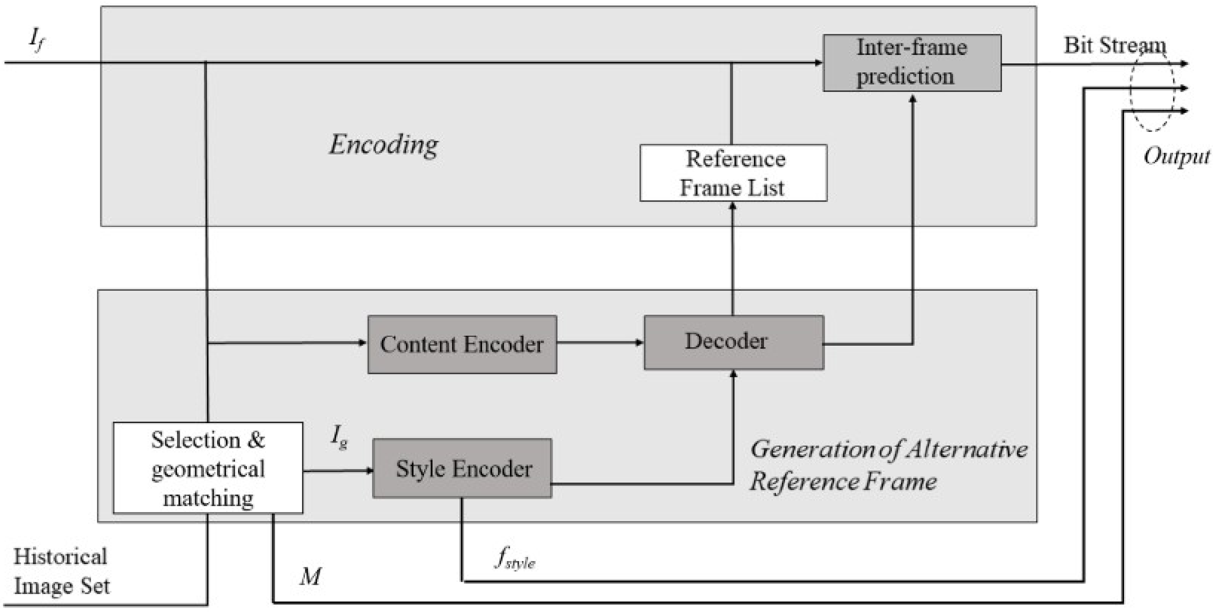

Figure 21 Framework of proposed coding scheme

This video compression scheme could be translated to work with modern mega EO satellite constellations as well, considering their very short revisit times and the fact that multiple satellites visit the same location albeit at different orbits.

As we have seen there has been several advances in image compression techniques both for general purpose use cases and satellite data compression which could be further exploited for satellite constellation data compression to achieve very high compression ratios and inherently more connected and smarter satellites. It is also worth mentioning that several of the ideas described above may not be directly applicable to practical scenarios where very low complexity is needed. Notwithstanding, many of these ideas will be valuable when designing the compression system due for this project.

INITIAL COMPRESSION EXPERIMENTS

A set of experiments have been run in order to assess compression performance and execution time trade-offs for several low-complexity compression algorithms. First, the properties of the test corpus are analyzed. Afterwards, compression performance results are discussed.

Test dataset properties

All experiments have been run on a set of 160 images provided by Satellogic. All images contain one component of 5120x5120 pixels, each of which contains 4 horizontal regions corresponding to different wavelengths. A distribution of the zero-order entropy of these images is shown next:

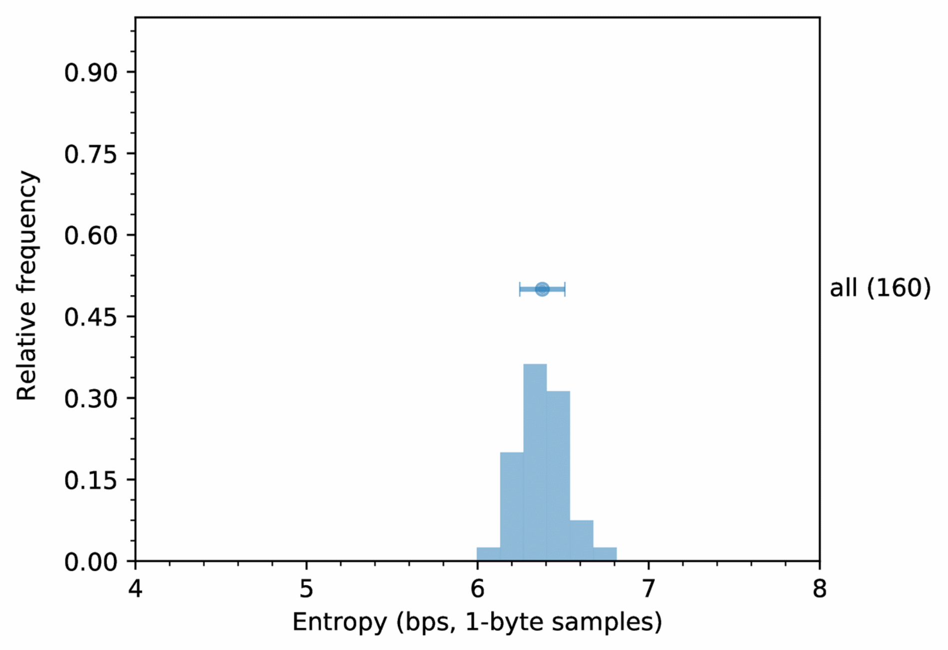

In addition to computing the entropy of all samples, the images are conceptually split into horizontal bands of 100% of the width. Some of these bands correspond to shadows produced by the optical filter. The following figure illustrates those areas, setting the content area to black:

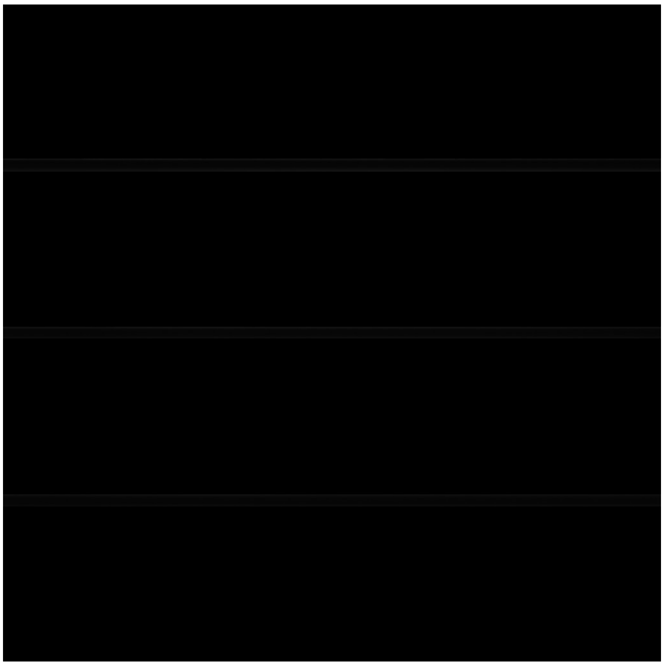

Another entropy-based metric is defined based on the content bands, referred to as *split content entropy*. This entropy corresponds to the sum of expected compressed bitrates of independent zero-order entropy coders, each one applied to a different band, and leaving the shadow regions uncoded. More specifically, the split content entropy is defined as the weighted (by area) entropy of each content band, divided by the total content area. A distribution of the split content entropy of the dataset is shown next.

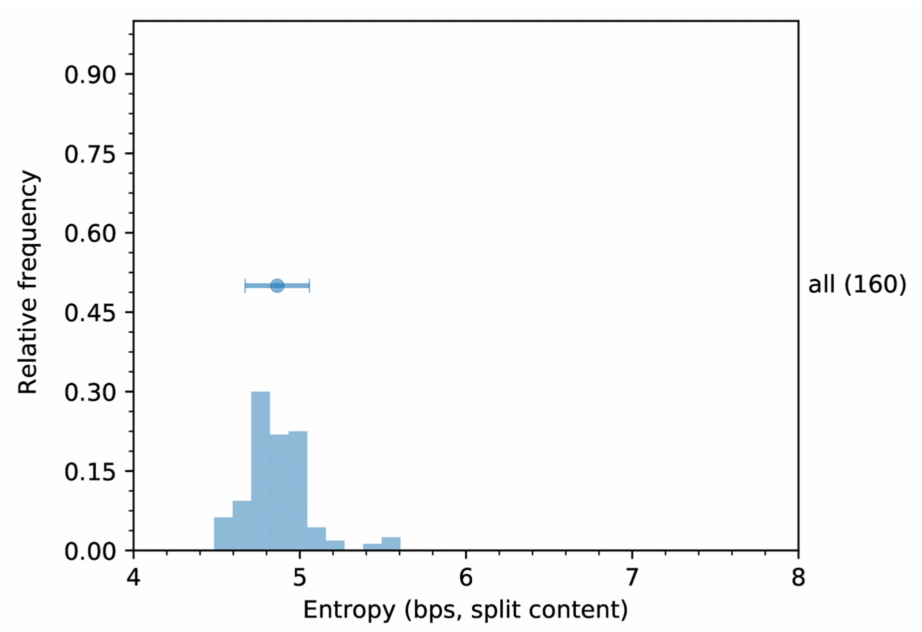

As can be observed, average entropy is blow 5 bits per sample (bps), while the original entropy was close to 6.5 bps, i.e., over 25% lower than the global entropy of the images. Note that the total area of the shadow region is only 5%. This suggests that compressing each content band separately may produce more efficient compression results.

Compression experiment results

Universal compressors

Several low-complexity universal lossless compressors, (zero-order and LZ-based) have been evaluated. In particular, 15 selected codecs from the TurboBench benchmark have been run on all test images on an Intel i5-8300h, 16GB ddr4 ram, 7200rpm HDD.

These tests include several types of compression pipelines, ranging from no entropy coding to more advanced ones with pattern matching and adaptive entropy coding. The following table provides compression efficiency results and execution time on the same platform.

Name	Compression ratio	Compression time (s)	Decompression time (s)
Brotli 11	2.19	66.87	0.139
Lzlib 9	2.18	16.166	0.633
Lzma 9	2.17	14.98	0.46
Lzham 4	2.15	17.737	0.192
Zstd 22	2.11	14.59	0.044
Lizard 19	1.53	2.323	0.02
Lizard 29	1.53	12.7	0.021
Lizard 39	1.53	2.364	0.025
Lizard 49	1.93	12.752	0.033
Lz4 9	1.51	0.939	0.01
Qlic 1	1.42	1.94	1.12

As can be observed, fast entropy coders applied directly to the images don't produce compression ratios much better than 2:1 (50% of the original size). It can also be observed that dictionary matching methods based on LZ are significantly slower than their non-LZ counterparts.

The average compression time and compressed image tabulated above are illustrated in the following figure. This figure includes results for JPEG-LS, a popular image compression codec.

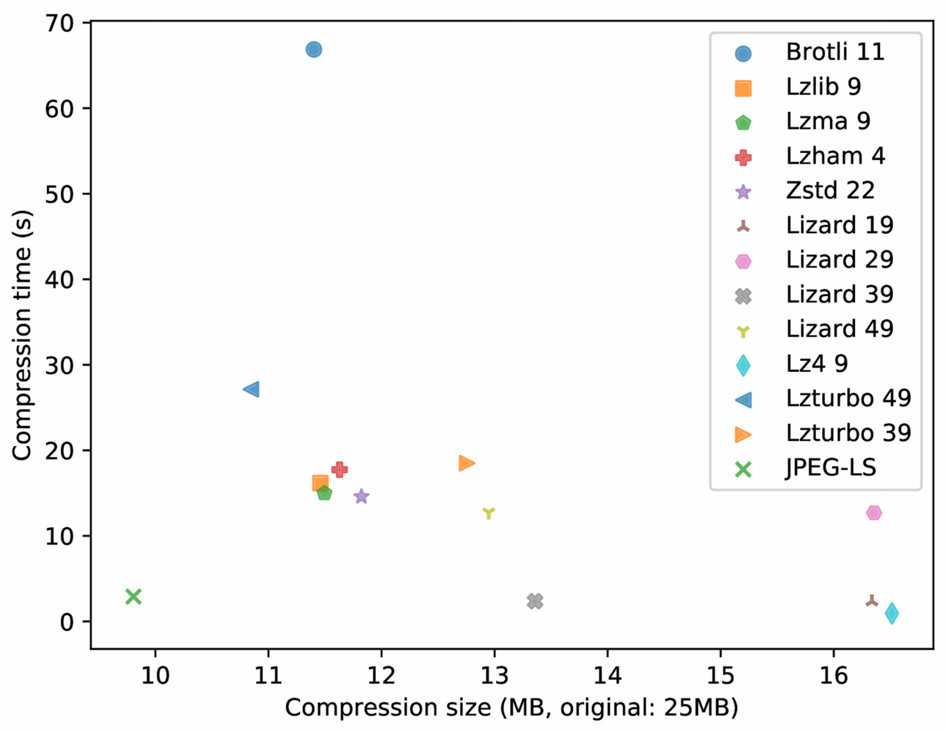

As can be observed, these families of codec are no match for JPEG-LS in either compression performance and execution time.

Image compression methods

A comparison of JPEG-LS and several other lossless image compressors is presented in this section. In this case, an AMD Ryzen Threadripper 1950X with 16GB of ram and SATA SSDs was used.

Several codecs were tested:

- FLIF, precursor of the JPEG-XL standard. Transform based, variable-to-variable entropy coder.
- JPEG-LS, prediction based with fixed-to-variable entropy coder.
- CCSDS 123.0-B-2, prediction based with different entropy coder modes, including fixed-to-variable and variable-to-variable entropy coders.
- Marlin, a compressor based on variable-to-variable (V2F) codes.

The following figure plots compression time and compressed data rate (in bits per pixel per component, bpppc).

As can be observed, the best compression performance is obtained by FLIF (basis for JPEG XL), but at a fairly high computational complexity. The CCSDS 123.0-B-2 entropy codecs and the JPEG-LS standard provide comparable compression-time trade-offs, with JPEG-LS being the fastest and the one producing larger compressed files.

On the other hand, Marlin provides much faster compression times (6-8 times faster) than JPEG-LS, while providing 18% higher compressed data rate.

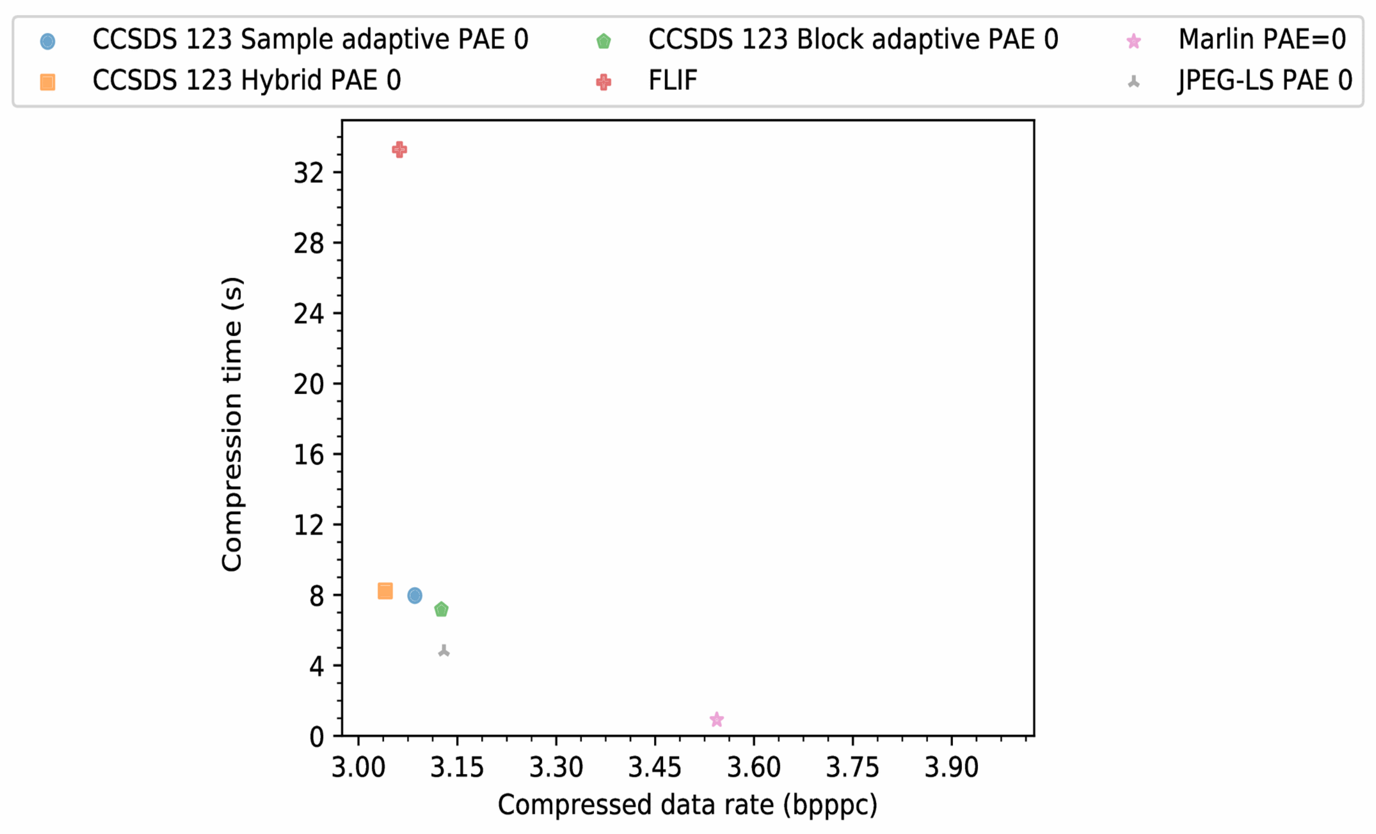

DISCUSSION AND FUTURE WORK

The properties of the test dataset have been analyzed. The filtered band structure of the images has been found to be significantly lower than that of the full images. This is an interesting line of attack, which can yield both compression performance improvements, and the possibility of dedicating fewer resources to estimating data statistics, since each band tends to be similar to itself.

Compression performance and execution time have been jointly analyzed for several representative LZ and image compression algorithms. In light of the discussed results, algorithms based on variable-to-fixed (V2F) codecs such as Marlin offer competitive compression performance (within 20% of the best-performing methods), with much faster compression times.

In light of these findings, the envised path of least resistance is original V2F compressor with custom decorrelation, and specific codes for each band type. This is recommended for the following reasons:

- Compression performance can still be improved with respect to Marlin's results shown above. because Marlin uses simple DPCM in its decorrelation stage. More advantageous prediction methods can be devised with acceptable impact on execution time.
- These decorrelation methods may include prediction based on other frames, among other approaches, and will be explored in the near future.
- The entropy coder of Marlin (Algorithm 7 in the following figures) is not optimal. Firstly, the V2F codes proposed by Yamamoto and Yokoo (solid pink line) provide results closer to the

theoretical limit (left figure) using a smaller footprint. Secondly, this smaller footprint can be used to use relatively larger dictionaries, which enhances overall performance (right figure).

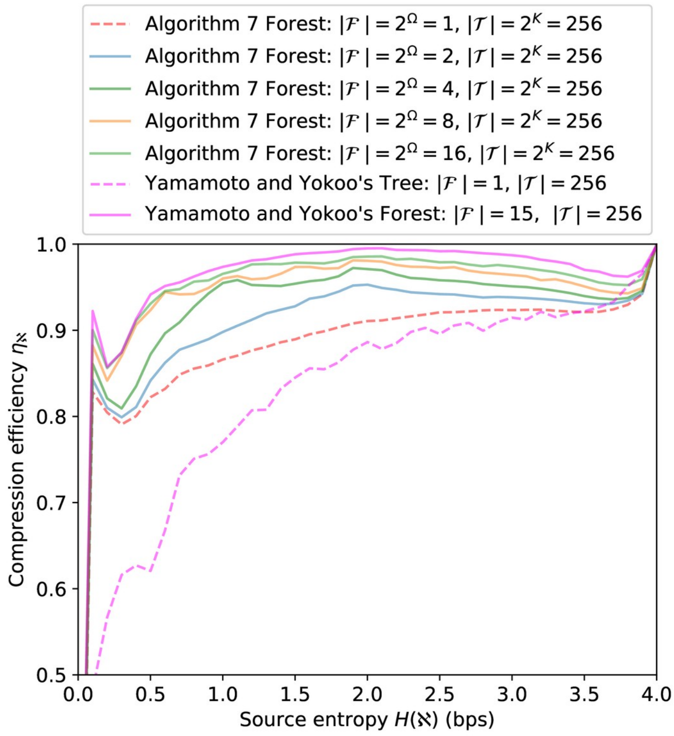

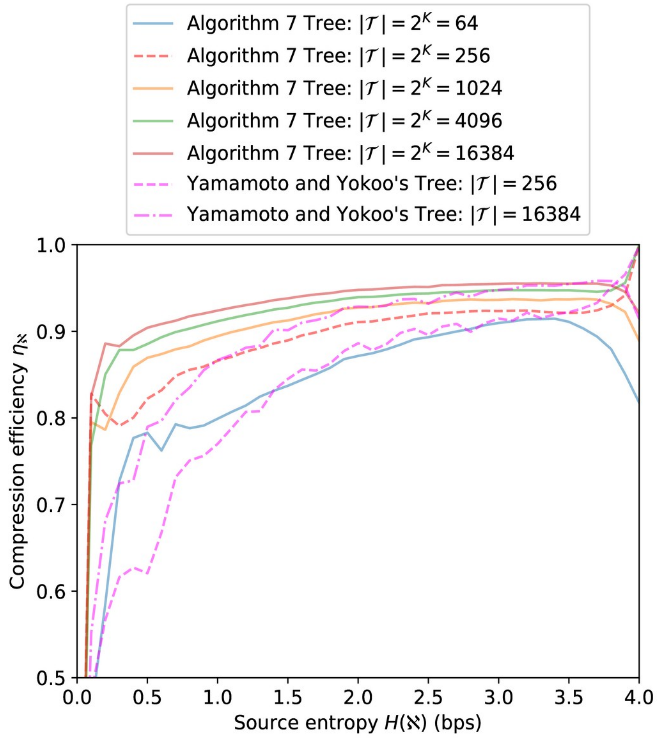

- This V2F skeleton can be easily extended to lossy compression. This will be developed in subsequent tasks of this project.

REFERENCES

[1] A. C. Clarke, “Extra-terrestrial relay,” in *Wireless World*, 1945, pp. 305–308.

[2] L. Wood, “Satellite Constellation Networks,” in *Internetworking and Computing Over Satellite Networks*, Springer US, 2003, pp. 13–34.

[3] “Satellites 101: LEO vs. GEO | Iridium Satellite Communications.” https://www.iridium.com/blog/2018/09/11/satellites-101-leo-vs-geo/ (accessed Apr. 23, 2020).

[4] R. Radhakrishnan, W. W. Edmonson, F. Afghah, R. M. Rodriguez-Osorio, F. Pinto, and S. C. Burleigh, “Survey of Inter-Satellite Communication for Small Satellite Systems: Physical Layer to Network Layer View,” IEEE Communications Surveys and Tutorials, vol. 18, no. 4. pp. 2442–2473, 2016, doi: 10.1109/COMST.2016.2564990.

[5] “Satellite constellation - Wikipedia.” https://en.wikipedia.org/wiki/Satellite_constellation (accessed Apr. 23, 2020).

[6] “Satellite constellation - Wikipedia.” https://en.wikipedia.org/wiki/Satellite_constellation#Design (accessed Apr. 13, 2020).

[7] S. W. Paek, S. Kim, and O. de Weck, “Optimization of reconfigurable satellite constellations using simulated annealing and genetic algorithm,” Sensors (Switzerland), vol. 19, no. 4, Feb. 2019, doi: 10.3390/s19040765.

[8] Klinkrad Heiner, Space Debris Models and Risk Analysis, 1st ed. Springer-Verlag Berlin Heidelberg, 2006.

[9] E. Stoll, H. Konstanski, C. Anderson, K. Douglass, and M. Oxfort, “The RapidEye constellation and its data products,” in IEEE Aerospace Conference Proceedings, 2012, doi: 10.1109/AERO.2012.6187173.

[10] “09. Communications – State of the Art of Small Spacecraft Technology.” https://sst-soa.arc.nasa.gov/09-communications (accessed Apr. 11, 2020).

[11] L. Wood, W. Ivancic, and K. P. Dörpelkus, “Using light-emitting diodes for intersatellite links,” in IEEE Aerospace Conference Proceedings, 2010, doi: 10.1109/AERO.2010.5446711.

[12] D. N. Amanor, W. W. Edmonson, and F. Afghah, Utility of Light Emitting Diodes for Inter-satellite Communication in Multi-Satellite Networks. 2016.

[13] F. Auli-Llinas, M. W. Marcellin, V. Sanchez, J. Serra-Sagrista, J. Bartrina-Rapesta, and I. Blanes, “Coding Scheme for the Transmission of Satellite Imagery,” in Data Compression Conference Proceedings, Dec. 2016, pp. 427–436, doi: 10.1109/DCC.2016.29.

[14] F. Aulí-Llinàs, M. W. Marcellin, V. Sanchez, J. Bartrina-Rapesta, and M. Hernández-Cabronero, “Dual Link Image Coding for Earth Observation Satellites,” IEEE Transactions on Geoscience and Remote Sensing, vol. 56, no. 9, pp. 5083–5096, Sep. 2018, doi: 10.1109/TGRS.2018.2806082.

[15] D. Zhou, M. Sheng, J. Luo, R. Liu, J. Li, and Z. Han, “Collaborative Data Scheduling with Joint Forward and Backward Induction in Small Satellite Networks,” IEEE Transactions on Communications, vol. 67, no. 5, pp. 3443–3456, May 2019, doi: 10.1109/TCOMM.2019.2900316.

[16] I. J. Goodfellow et al., “Generative Adversarial Nets.” [Online]. Available: http://www.github.com/goodfeli/adversarial.

[17] “Understanding Variational Autoencoders (VAEs) - Towards Data Science.” https://towardsdatascience.com/understanding-variational-autoencoders-vaes-f70510919f73 (accessed Jun. 15, 2020).

[18] A. Razavi, A. van den Oord, and O. Vinyals DeepMind, “Generating Diverse High-Fidelity Images with VQ-VAE-2.” [Online]. Available: https://github.com/deepmind/sonnet/blob/master/sonnet/python/modules/nets/vqvae.py.

[19] A. Gonzalez-Garcia, J. van de Weijer, and Y. Bengio, “Image-to-image translation for cross-domain disentanglement.” [Online]. Available: https://github.com/agonzgarc/cross-domain-disen.

[20] E. Sanchez, M. Serrurier, and M. Ortner, “Learning Disentangled Representations of Satellite Image Time Series,” Mar. 2019, Accessed: May 01, 2020. [Online]. Available: http://arxiv.org/abs/1903.08863.

[21] L. Wu, K. Huang, and H. Shen, “A GAN-based Tunable Image Compression System.”

[22] Z. Cui, J. Wang, B. Bai, T. Guo, Y. Feng, and † Huawei, “G-VAE: A CONTINUOUSLY VARIABLE RATE DEEP IMAGE COMPRESSION FRAMEWORK.”

[23] M. Li, J. Lin, Y. Ding, Z. Liu, J.-Y. Zhu, and S. Han, “GAN Compression: Efficient Architectures for Interactive Conditional GANs Figure 1.”

[24] L. Liao, J. Xiao, Y. Li, M. Wang, and R. Hu, “Learned Representation of Satellite Image Series for Data Compression,” Remote Sensing, vol. 12, no. 3, p. 497, Feb. 2020, doi: 10.3390/rs12030497.